Exp. Theo. NANOTECHNOLOGY 10 (2026) 1093-1107 https://doi.org/10.56053/10.S.1093

Strengthening of aluminum piston alloy through Al_2O_3 nanoparticles incorporation

Haitham Mohammed Ibrahim Al-Zuhairi[1,*], *Iqbal alshalal*[1], *Hind H. Abbood*[1], *M. Al Nuaimi*[2]

[1]Training and Workshop Center/ University of Technology- Iraq, Baghdad, Iraq
[2]College of Applied Sciences, University of Technology- Iraq, Baghdad, Iraq
[*]) Email: haitham.m.ibrahim@uotechnology.edu.iq

Received 22/1/2026, *Received in revised form* 23/4/2026, *Accepted* 29/4/2026, *Published* 15/5/2026

Aluminum alloys are widely utilized in piston manufacturing for internal combustion engines due to their high thermal conductivity, low density, and excellent machinability. However, their relatively moderate mechanical strength limits performance under severe operating conditions. In this study, the mechanical properties of an aluminum piston alloy (EN AB-47100, AlSi12Cu1) are enhanced through the incorporation of Al_2O_3 NPs as reinforcement. Composites are fabricated using the stir casting technique with Al_2O_3 NP additions of 2 wt.%, 4 wt.%, and 6 wt.%. The influence of reinforcement content on tensile strength, hardness, and impact strength is systematically investigated. The results showed that the tensile strength increased from approximately 180 MPa for the base alloy to 220 MPa and reached a maximum of 255 MPa at 4 wt.% Al_2O_3 NPs, followed by a decrease to 230 MPa at 6 wt.%. Similarly, hardness values increased progressively with reinforcement, achieving maximum improvement at 4 wt.% due to enhanced resistance to localized plastic deformation. The impact strength also improved from about 5.5 J for the base alloy to 7.6 J at 4 wt.% reinforcement, indicating better energy absorption capability, before decreasing at 6 wt.% due to increased brittleness. The observed improvements are attributed to effective load transfer, dislocation hindrance, Orowan strengthening, and grain refinement resulting from the uniform dispersion of Al_2O_3 NPs. However, excessive reinforcement (6 wt.%) led to nanoparticle agglomeration, increased porosity, and weak interfacial bonding, which negatively affected the mechanical performance. The findings indicate that 4 wt.% Al_2O_3 NPs is the optimal reinforcement level, providing the best combination of tensile strength, hardness, and impact resistance. These results highlight the potential of Al–Al_2O_3 NP composites for enhanced performance and durability in piston applications under demanding service conditions.

Keywords: Al_2O_3 NPs; Aluminum matrix composites; Piston alloy; Mechanical.

1. INTRODUCTION

In internal combustion engines, pistons are very important parts of the engine. Traditionally, pistons are made from cast iron because of its strength and ability to stand up under wear. However, advances in material engineering have made aluminum-silicon (Al-Si) alloys a commonly used material in making pistons. Al-Si alloys provide many benefits, such as low density, great thermal conductivity, excellent machining properties, and the ability to use less fuel than other materials. When compared to conventional materials that have not been reinforced, Al-Si-Mg alloys exhibit exceptional performance (e.g., strength, stiffness, and thermal stability) and are used as the preferred material for many various types of alloys. Recent developments in aluminum matrix composites (AMCs) have created renewed interest in using these composite materials due to their combination of aluminum alloy matrices and ceramic materials. This unique combination of materials produces composite materials that have improved mechanical characteristics and tribological properties. Some studies have demonstrated that if alumina nanoparticles are used as a reinforcing element in AMCs, the resulting composites will exhibit improved hardness, strength, and resistance to wear. Ceramic materials, because of their high melting point and ability to sustain heat for long periods gives these materials great use in applications where high temperatures and heavy mechanical loads will be applied to ceramic materials [23-25]. There are two primary ways in which the processing parameters affect the manufacturing of composite materials; they are: processing parameters (i.e., stir casting and other similar techniques) and particle distribution, microstructure and overall mechanical behavior of composite materials can be influenced. Among these parameters, stir speed, temperature and time are key parameters [31-35].

Early research has established that selecting and using the correct processing parameters will enhance the quality of the materials, whereas improper handling of the composite materials during processing (e.g., agglomeration of particles) or failing to prevent defects during the manufacturing of composite engine products will negatively affect the products' performance. As a result, there has been a demand for higher strength-to-weight ratios compared to metals for engine parts made from composite materials. According to the literature, the alloy AlSi12 offers a suitable compromise between the thermal and mechanical properties of metallic engine components. Aluminum-based alloys have many flaws when exposed to harsh conditions like high load and temperature. Alumnium alloys, such as AlSi12 have similar problems with wear and fracture when they are used multiple times at fast rates. Researchers will need to investigate ways to improve the mechanical properties of aluminum alloys as a way of increasing their durability and performance. Advances in research may make it more likely that goals will be realized. The fundamental weakness in the material to resist deformation and wear after prolonged periods of use is due to the lack of discontinuity in the iMatrix [54]. Uses of alumina as a reinforcing material in the production of aluminum composites is common because of the high level of strength, exceptional thermal stability and the inert nature of alumina [55]. Due to the very high melting point of approximately 2000 °C, Al_2O_3 NP's are able to effectively withstand conditions that cause damage from heat and mechanical forces [56]. The addition of Al_2O_3 nanoparticles (NPs) to a material can increase its load transfer capabilities, limit the movement of dislocations and increase the resistance of that material to plastic deformation [57]. Therefore, aluminium NPs that are reinforced with Al_2O_3 will provide an increase in hardness, tensile strength and wear resistance, thereby making composites suitable for piston applications [58]. There has been considerable research on the interface between aluminium matrix (45$$) composites and ceramic particles; however, there has not been a

focused study on optimizing the mechanical properties of AlSi12Cu1 (EN AB-47100) pistons with different controlled weight percentages of Al_2O_3 NPs. Previous studies have also shown that the relationship between the mechanical performance of composite materials is a result of both the degree of reinforcement and the1629083854.9073% (or more) level of reinforcement and those future studies should continue to explore these relationships to the point of determining what is optimal and beyond the maximum load of composites [59]. Identification of motivations for additional exploration is based on practical issues such as the fact that automotive pistons have cracked while under detonation conditions as a result of the use of low-octane fuel [60]. The reason for conducting this research is due to some real world concerns related to instances of cracked pistons in automotive engines when detonation occurs due to using low-octane gasoline. Detonation typically creates high pressures and temperatures, which create high levels of thermal stress, which results in cracked piston crowns and other types of damage. An example of one of these damaged pistons is shown in Figure 1.

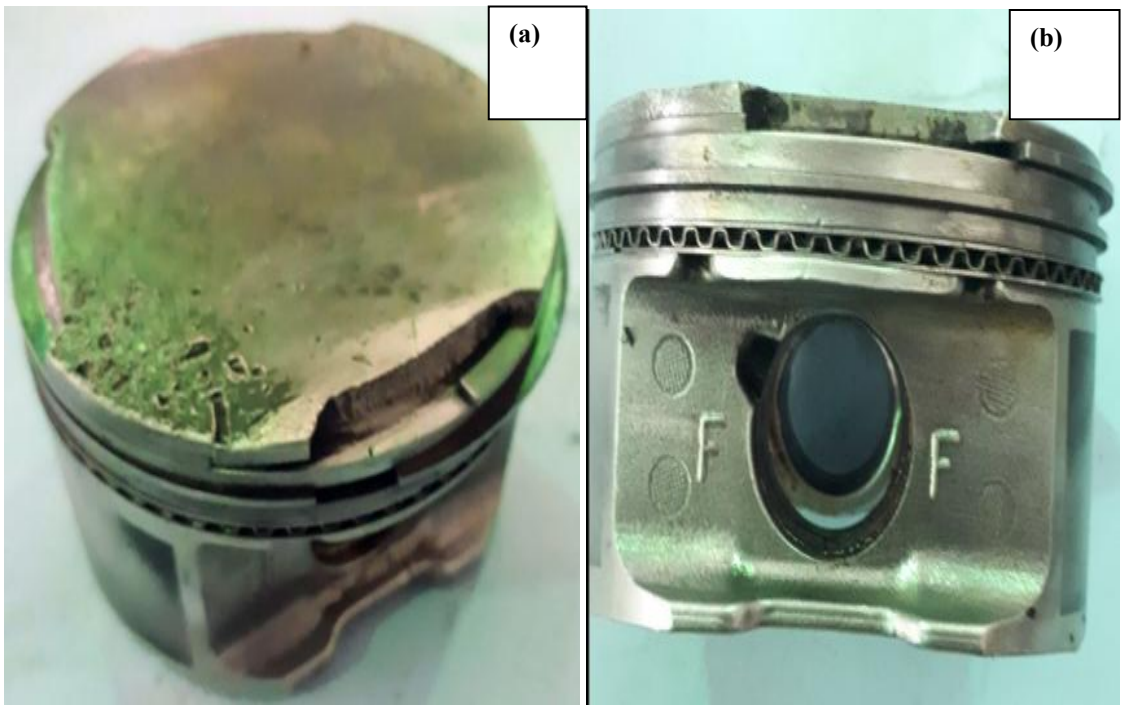

Figure 1. (a) Top view of the damaged aluminum piston showing crack formation and material degradation at the piston crown; (b) side view of the piston illustrating the overall geometry and condition of the skirt and pin bore region.

Enhancing the mechanical properties of piston materials is therefore essential to reduce failure and improve reliability [61]. The objective of this study is to enhance the mechanical performance of an aluminum piston alloy through the incorporation of Al_2O_3 NPs using the stir casting technique [62]. Specifically, the work focuses on fabricating Al– Al_2O_3 NP composite materials with varying reinforcement levels of 2 wt.%, 4 wt.%, and 6 wt.% in order to systematically investigate the influence of particle content on mechanical behavior [63]. The study aims to evaluate key properties, namely tensile strength and hardness, to assess the effectiveness of alumina reinforcement in strengthening the aluminum matrix [64]. Furthermore, the research seeks to determine the optimal weight percentage of Al_2O_3 NPs that provides the best balance of improved mechanical properties without introducing

detrimental effects such as particle agglomeration or structural defects [65]. Ultimately, the findings are intended to support the development of more durable and high-performance piston materials for internal combustion engine applications [66]. In this paper, aluminum piston alloy EN AB-47100 (AlSi12Cu1) is reinforced with Al_2O_3 nanoparticles (NPs) using the stir casting technique. The influence of varying reinforcement content on tensile strength and hardness is experimentally investigated, and the optimal composition for enhanced mechanical performance in piston applications is determined.

2. MATERIALS WORK

The master alloy used in this study is prepared from recycled piston scrap obtained from USA Chrysler Jeep engines. The chemical composition of the alloy is determined in accordance with ASTM E1251 standard at the Central Organization for Standardization and Quality Control (COSQC). The analyzed chemical composition of the as-received piston alloy is presented in Table 1.

Table 1 Chemical composition of the master aluminum piston alloy (EN AB-47100) used in this study (wt.%).

Item number	%	element
1	11.8	Si
2	0.596	Fe
3	1.29	Cu
4	0.305	Mn
5	1.13	Mg
6	0.335	Zn
7	0.0325	Cr
8	0.744	Ni
9	0.157	Ti
10	0.0173	Pb
11	0.0700	p
12	0.02	V
others	0.0176	-
13	Reminder	Al

A pit furnace running at about 800 °C is used to complete the melting process as shown in Figure 2. The scrap material from pistons is melted in a crucible until it is completely melted. To ensure the quality of the castings and to minimize thermal defects, the molten metal is poured into a pre-heated iron mold (at 400 °C) before being cast. The pre-heating of the mold decreases thermal gradients, avoids premature solidification, and improves the surface appearance of the castings. After casting, the material produced is in cylindrical bars with a length of approximately 250 mm and a diameter of approximately 15 mm [67]. These cast bars formed the matrix (base) alloy used for making composite samples for mechanical evaluation. The chemical composition in Table 1 verifies that the composite sample's base alloy has an Al–Si-based piston alloy composite of AlSi12Cu1-type (EN AB-47100). Having greater than 10% silicon will aid in anti-wear along with providing lower thermal expansion. Both are critical requirements for pistons. Both copper (1.29%) and magnesium (1.13%) will aid in strength enhancement from precipitation hardening methods. Nickel (0.744%) adds strength and thermal stability to the material with respect to use at elevated temperatures; therefore, it is essential

for engine parts. Various minor alloying elements (manganese, chromium, and titanium) promote refined grain structure and enhanced mechanical property characteristics while iron content (0.596%) could affect the generation of intermetallics which could create a brittle material for this alloy system. This alloy composition would be well suited for high-temperature, high-load applications on pistons [68].

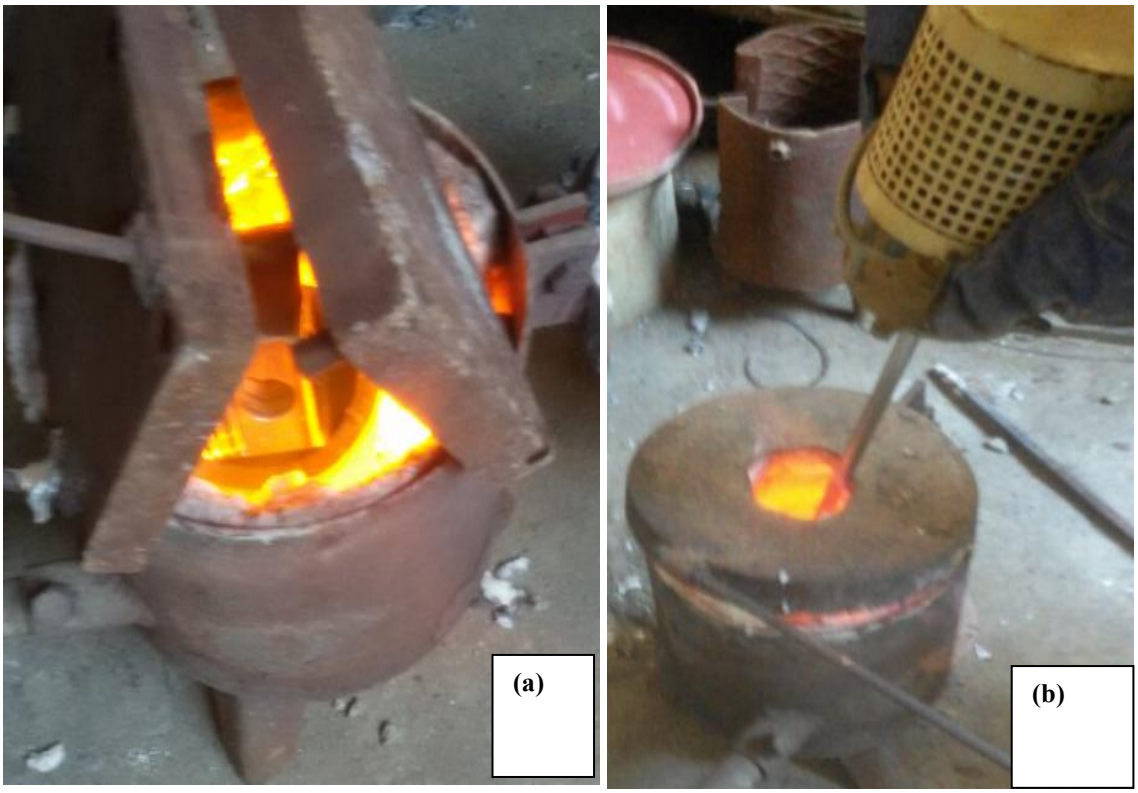

Figure 2 (a) Melting process of recycled aluminum piston scrap in a pit furnace at 800 °C prior to casting; (b) mechanical stirring of Al_2O_3 NPs within the molten aluminum matrix to ensure uniform particle distribution during composite fabrication.

2.1. Composite fabrication (incorporation of Al_2O_3 NPs)

Due to the straightforward, low-cost, and large-scale production capabilities of stir casting, Al−A2O3 (NP) composites are manufactured using this process. As described in Section 2, the EN AB-47100 as-cast aluminum piston alloy is melted down in a pit furnace to create a completely molten material at around 800 °C. The A2O3 NPs used to reinforce the composite had an average particle size of 25 nm. Before they are added to the melting aluminum, the nanoparticles are heated to approximately 300 °C to 400 °C to dry them out and allow for better interaction with the melting aluminum. Once dry, the A2O3 nanoparticles are introduced into the melt by weight percent (2%, 4%, and 6%) in an incremental manner. A mechanical stirrer coated with graphite is used to mix the material, maintaining a constant speed to achieve dispersion and limit agglomeration of the nanoparticles during the mixing process. By creating a vortex through the molten metal due to stirring, it is possible to effectively incorporate and distribute A2O3 NPs throughout the aluminum matrix. Excessive turbulence is avoided in order to prevent gas entrapment and formation of porosity. After a homogenous mixture is achieved, the composite melt is poured into an iron mold that is pre-heated to around 400 °C to

produce cylindrical cast specimens of the composite. The cast composites are allowed to cool at room temperature, and then are subsequently machined into standard size test specimens to perform mechanical characterization. The Al-A2O3 NP composites are then tested for tensile strength and hardness to determine how well the addition of nanoparticles would affect the mechanical performance of the Al Piston Alloy composite material. [69,70].

2.2. Tensile test

According to standard specifications in fig 3(a) [1]. The specimens comprised five different samples based on the composition. Only one is made from base alloy (unreinforced) while the other three had varying amounts (2 wt, 4wt., etc.) of Al_2O_3 NPs dispersed throughout them. Each specimen had cylindrical shape with gauge diameter of 10 mm and total length of 100 mm. Machining is done so that all specimens are the same size, shape, and finish in accordance with ASTM E8. Tensile testing determined the ultimate tensile strength (using Universal Testing Machines [Type Instron] as shown below) is performed at room temperature using a constant crosshead speed of 10 mm per minute. Throughout the testing, the load and elongation are recorded for data analysis of the tensile properties of both the base alloy and fabricated composites. The resulting values from this study are used to assess how mechanical properties of the aluminum piston alloy are affected by Al_2O_3 nanoparticle reinforcements. [71].

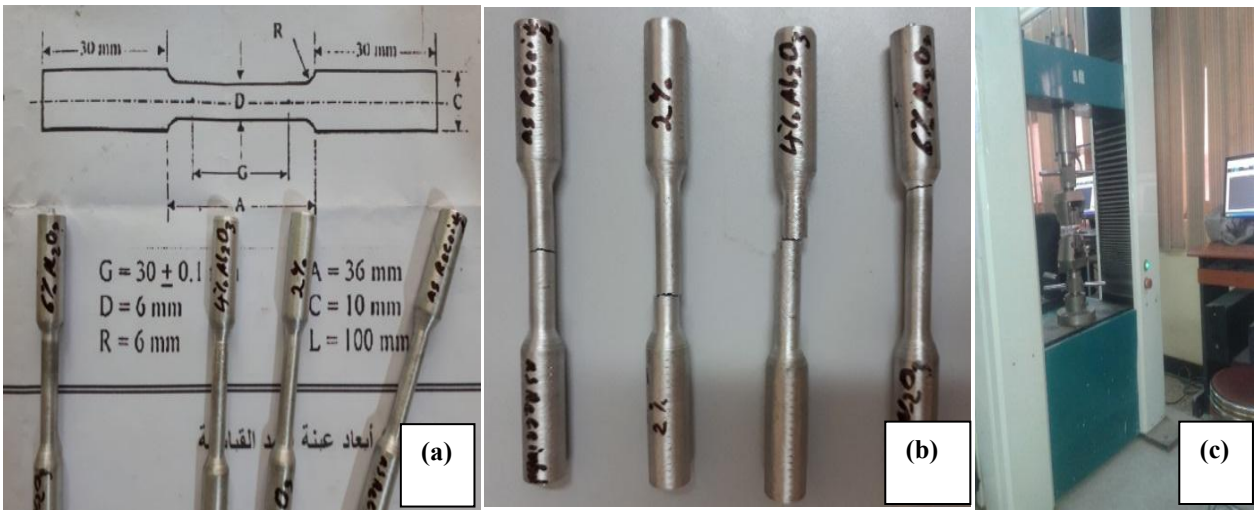

Figure 3 (a) Standard dimensions of tensile test specimen according to ASTM E8; (b) prepared tensile specimens with varying Al_2O_3 NPs content (0 wt.%, 2 wt.%, 4 wt.%, and 6 wt.%); (c) universal testing machine (Instron) used for conducting tensile tests.

2.3. Hardness test

The hardness of the base alloy and the fabricated Al– Al_2O_3 (NP) composites is evaluated using a Vickers hardness testing machine, as shown in Figure 4(a). The tests are conducted under a load of 60 kgf with an appropriate dwell time to ensure reliable indentation measurements. Four specimens are prepared for hardness evaluation, corresponding to the different compositions: the base alloy (as-received), and composites reinforced with 2 wt.%, 4 wt.%, and 6 wt.% Al_2O_3 NPs. Each specimen is machined into cylindrical discs with dimensions of approximately 12 mm in diameter and 9 mm in

thickness. Prior to testing, the specimen surfaces are ground and polished to obtain a smooth and flat surface, ensuring accurate indentation readings. Multiple indentations are taken on each specimen to improve measurement accuracy, and the average hardness value is recorded. The hardness test is performed to assess the resistance of the material to localized plastic deformation and to evaluate the effect of Al_2O_3 NP reinforcement on the mechanical behavior of the aluminum matrix. The hardness of the aluminum piston alloy is expected to increase with the addition of Al_2O_3 nanoparticles due to the presence of hard ceramic reinforcement within the matrix. These NPs act as obstacles to dislocation movement, thereby increasing resistance to plastic deformation. Additionally, the uniform dispersion of Al_2O_3 NPs enhances load-bearing capability and contributes to improved surface hardness. However, at higher reinforcement levels (e.g., 6 wt.%), a possible reduction or plateau in hardness may occur due to nanoparticle agglomeration and increased porosity, which can negatively affect the material's integrity. Therefore, an optimal reinforcement content is expected, where hardness improvement is maximized without introducing defects [72].

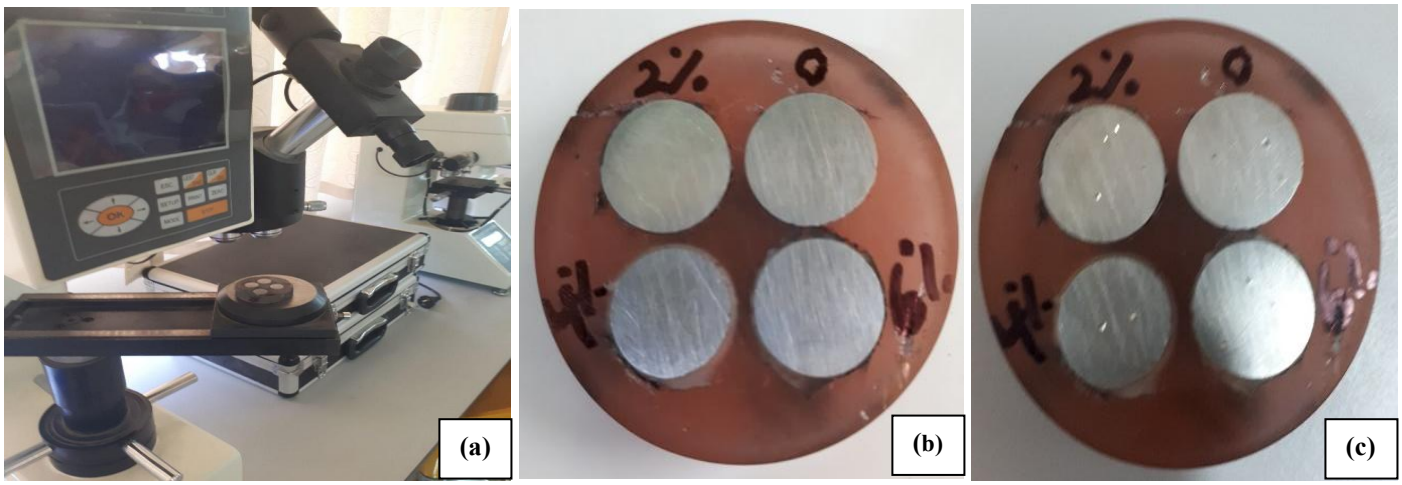

Figure 4 (a) Vickers hardness testing machine used for evaluating the hardness of the specimens; (b) prepared samples of the base alloy and Al–Al_2O_3 NP composites (0 wt.%, 2 wt.%, 4 wt.%, and 6 wt.%) before testing; (c) specimens after hardness testing showing indentation marks.

2.4. Impact test

Impact strength of the base alloy and Al–Al_2O_3 NP composites is evaluated to determine the ability of the materials to absorb energy under sudden loading conditions. Four specimens are prepared, corresponding to the base alloy and composites reinforced with 2 wt.%, 4 wt.%, and 6 wt.% Al_2O_3 NPs. The test may be conducted using a Charpy impact testing machine according to ASTM E23. The absorbed impact energy is recorded for each specimen, and the impact strength is calculated based on the fractured cross-sectional area of the sample [73].

1. RESULTS AND DISCUSSION

3.1.Tensile strength behavior of Al–Al_2O_3 NP composites

The variation of tensile strength with Al_2O_3 NP content is illustrated in Figure 5. It is observed that the tensile strength of the aluminum piston alloy increases significantly with the addition of Al_2O_3 NPs up to 4 wt.%, followed by a decrease at 6 wt.%. The base alloy exhibits a tensile strength of approximately 180 MPa, which increases to 220 MPa and reaches a maximum value of 255 MPa at 4 wt.% Al_2O_3 NPs. However, a reduction to 230 MPa is observed at 6 wt.% reinforcement. The enhancement in tensile strength up to 4 wt.% Al_2O_3 NPs is primarily attributed to effective load transfer between the aluminum matrix and the uniformly dispersed nanoparticles. The presence of Al_2O_3 NPs restricts dislocation motion, thereby increasing resistance to plastic deformation. Additionally, the fine particle distribution contributes to grain refinement, further improving mechanical strength. At 4 wt.% reinforcement, the composite achieves optimal performance due to a balanced distribution of nanoparticles within the matrix. However, further addition to 6 wt.% leads to a decline in tensile strength. This behavior is associated with nanoparticle agglomeration, poor wettability, and increased porosity. These defects act as stress concentration sites, promoting crack initiation and reducing load-bearing capacity [74].

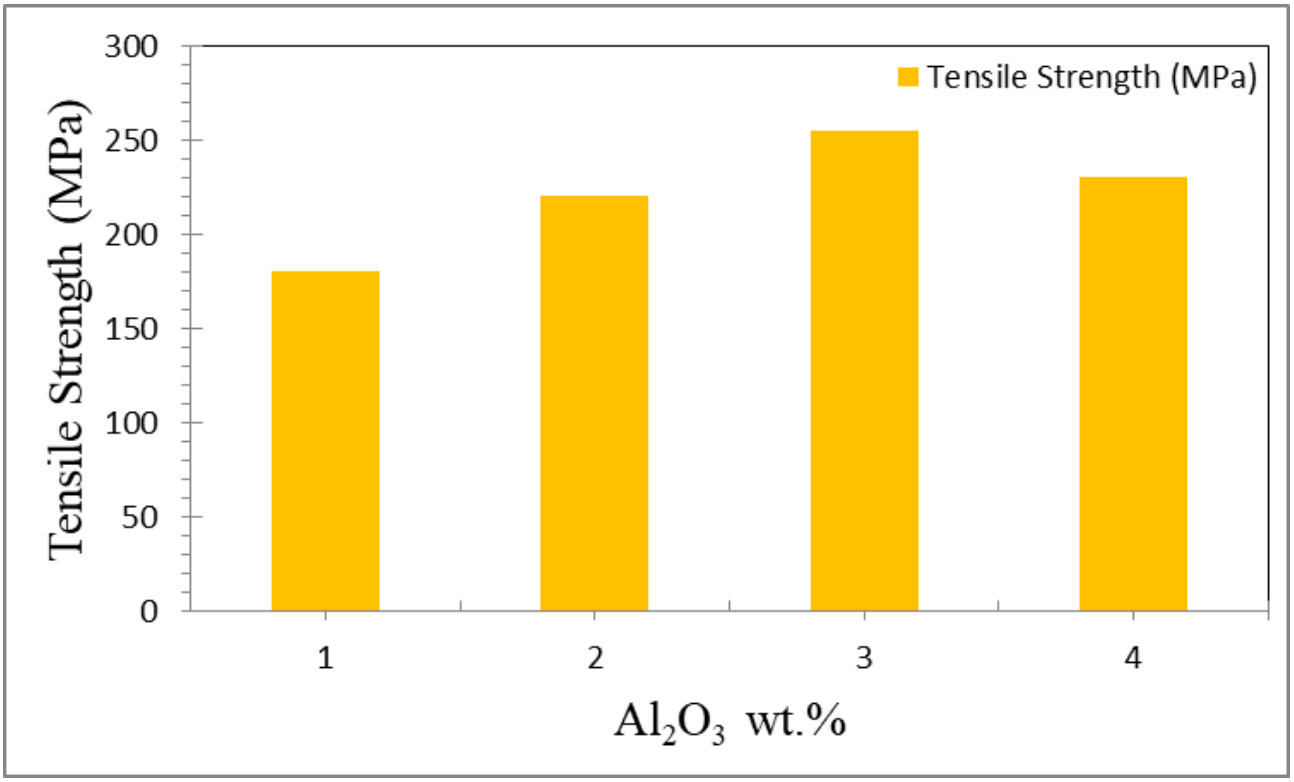

Figure 5 Variation of tensile strength of Al–Al_2O_3 nanoparticle (NP) composites as a function of reinforcement content (0 wt.%, 2 wt.%, 4 wt.%, and 6 wt.%).

3.1.1. Effect of Al_2O_3 NPs weight fraction on tensile strength

The effect of Al_2O_3 NPs weight fraction on tensile strength is shown in Figure 6. The tensile strength increases from the base alloy to 4 wt.% Al_2O_3 NPs, then decreases at 6 wt.% due to possible nanoparticle agglomeration and porosity.

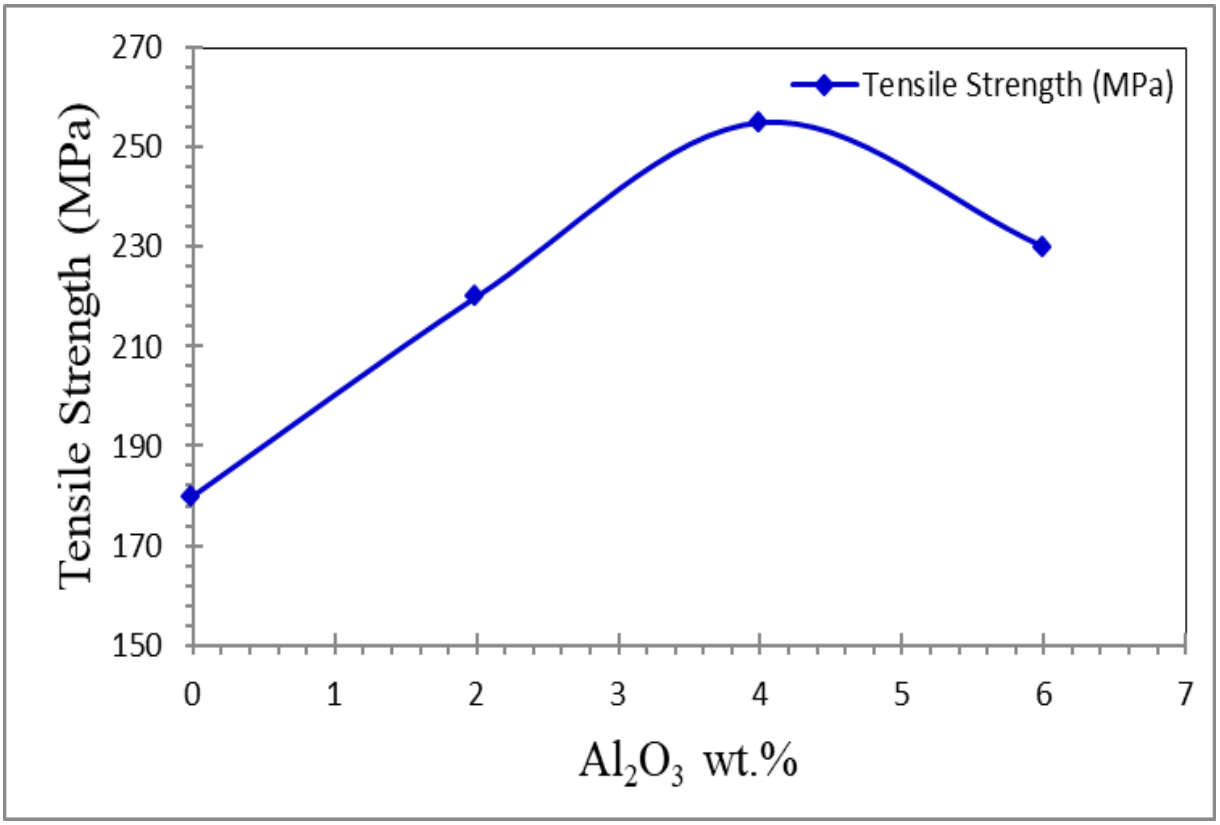

Figure 6 Variation of tensile strength of Al– Al_2O_3 NP composites with different Al_2O_3 NP weight fractions, showing maximum tensile strength at 4 wt.% reinforcement.

3.1.2. Strengthening mechanisms in reinforced aluminum matrix

The improvement in tensile strength of the Al–Al_2O_3 NP composites can be attributed to several fundamental strengthening mechanisms operating simultaneously within the aluminum matrix. The presence of hard ceramic nanoparticles introduces barriers to dislocation motion, thereby enhancing the overall mechanical performance of the composite. One of the primary mechanisms is load transfer strengthening, where the applied stress is partially transferred from the ductile aluminum matrix to the high-strength Al_2O_3 NPs. This mechanism is effective when there is good interfacial bonding between the matrix and the reinforcement, allowing the nanoparticles to carry a portion of the applied load and thereby increasing the tensile strength of the composite. Another significant mechanism is dislocation strengthening, in which the Al_2O_3 NPs act as obstacles to dislocation movement. The accumulation of dislocations around the nanoparticles increases the internal stress required for plastic deformation. In addition, the mismatch in thermal expansion coefficients between aluminum and Al_2O_3 NPs during

solidification leads to the generation of geometrically necessary dislocations, further contributing to strengthening. The Orowan strengthening mechanism also plays an important role, particularly due to the nanoscale size of the reinforcement particles. In this mechanism, dislocations bow around the nanoparticles, forming loops that require higher applied stress for continued deformation. This effect becomes more pronounced with finer particle sizes and uniform dispersion. Furthermore, the addition of Al_2O_3 NPs contributes to grain refinement of the aluminum matrix. The presence of nanoparticles during solidification acts as nucleation sites, resulting in a finer grain structure. According to the Hall–Petch relationship, smaller grain sizes lead to increased strength due to the higher resistance to dislocation movement across grain boundaries. Despite these beneficial mechanisms, excessive addition of nanoparticles (e.g., 6 wt.%) can lead to adverse effects such as particle agglomeration and increased porosity. These defects reduce the effectiveness of load transfer and create stress concentration sites, which ultimately diminish the tensile strength of the composite. The combined effect of load transfer, dislocation strengthening, Orowan looping, and grain refinement is responsible for the observed enhancement in tensile strength of Al– Al_2O_3 NP composites, with optimal performance achieved at moderate reinforcement levels [10, 11].

3.1.3. Degradation of tensile strength at higher reinforcement (6 wt.%)

Although the addition of Al_2O_3 NPs enhances the tensile strength of the aluminum matrix at lower reinforcement levels, a noticeable reduction in strength is observed at higher content (6 wt.%). This decline in tensile performance is primarily attributed to microstructural defects introduced at excessive nanoparticle concentrations. At higher weight fractions, Al_2O_3 NPs tend to agglomerate due to their high surface energy and strong interparticle attraction. These agglomerated clusters lead to a non-uniform distribution of reinforcement within the aluminum matrix, which disrupts effective load transfer and reduces the overall strengthening efficiency. Instead of acting as strengthening sites, these clusters behave as weak regions within the composite. Additionally, the increased particle content can negatively affect the wettability between the aluminum matrix and the nanoparticles during the stir casting process. Poor wettability results in inadequate bonding at the matrix–particle interface, which weakens the interfacial strength and limits stress transfer under tensile loading. Another critical factor contributing to the reduction in tensile strength is the formation of porosity. At higher reinforcement levels, the stirring process may trap gases and introduce voids into the molten metal. These pores act as stress concentration sites, promoting crack initiation and accelerating fracture under applied load. Furthermore, the presence of excessive nanoparticles increases the likelihood of microcrack initiation at particle–matrix interfaces, especially in regions with clustered particles. This leads to premature failure of the composite, thereby reducing its tensile strength compared to the optimally reinforced material. In comparison with lower reinforcement levels, particularly the 4 wt.% composite, the 6 wt.% Al_2O_3 NP composite exhibits inferior mechanical performance despite the higher particle content. This clearly indicates that there exists an optimal reinforcement level, beyond which the detrimental effects of agglomeration, porosity, and poor interfacial bonding outweigh the benefits of nanoparticle strengthening [20,21].

3.2. Hardness characteristics of Al–Al_2O_3 NP composites

The hardness behavior of the aluminum piston alloy reinforced with Al_2O_3 NPs is an important indicator of its resistance to localized plastic deformation and wear performance. The variation of hardness with different Al_2O_3 NP weight fractions is presented in Figure 7. It is observed that the hardness of the composite increases progressively with the addition of Al_2O_3 NPs up to 4 wt.%, followed by a slight reduction at 6 wt.% reinforcement. The base alloy exhibits the lowest hardness

due to the absence of reinforcing particles. With the incorporation of 2 wt.% Al_2O_3 NPs, a noticeable improvement in hardness is observed, which further increases significantly at 4 wt.% reinforcement. This enhancement is primarily attributed to the presence of hard ceramic nanoparticles uniformly distributed within the aluminum matrix. These nanoparticles act as obstacles to plastic deformation by resisting indentation and restricting dislocation movement. At 4 wt.% Al_2O_3 NP content, the composite demonstrates maximum hardness, indicating an optimal dispersion of nanoparticles and strong interfacial bonding between the matrix and reinforcement. The improved hardness at this composition can also be associated with increased resistance to micro-plastic deformation and enhanced load-bearing capacity of the composite surface. However, at higher reinforcement content (6 wt.%), a slight decrease or saturation in hardness is observed. This behavior can be explained by nanoparticle agglomeration and increased porosity within the matrix. These defects reduce the effective contact area during indentation and lead to localized stress concentrations, thereby lowering the hardness compared to the optimal composition. The results demonstrate that the hardness of Al– Al_2O_3 NP composites is strongly dependent on the reinforcement content, with 4 wt.% identified as the optimal level for achieving maximum hardness. The observed trend is consistent with the tensile strength behavior, confirming the effectiveness of Al_2O_3 NPs in enhancing the mechanical performance of aluminum piston alloys [31, 43].

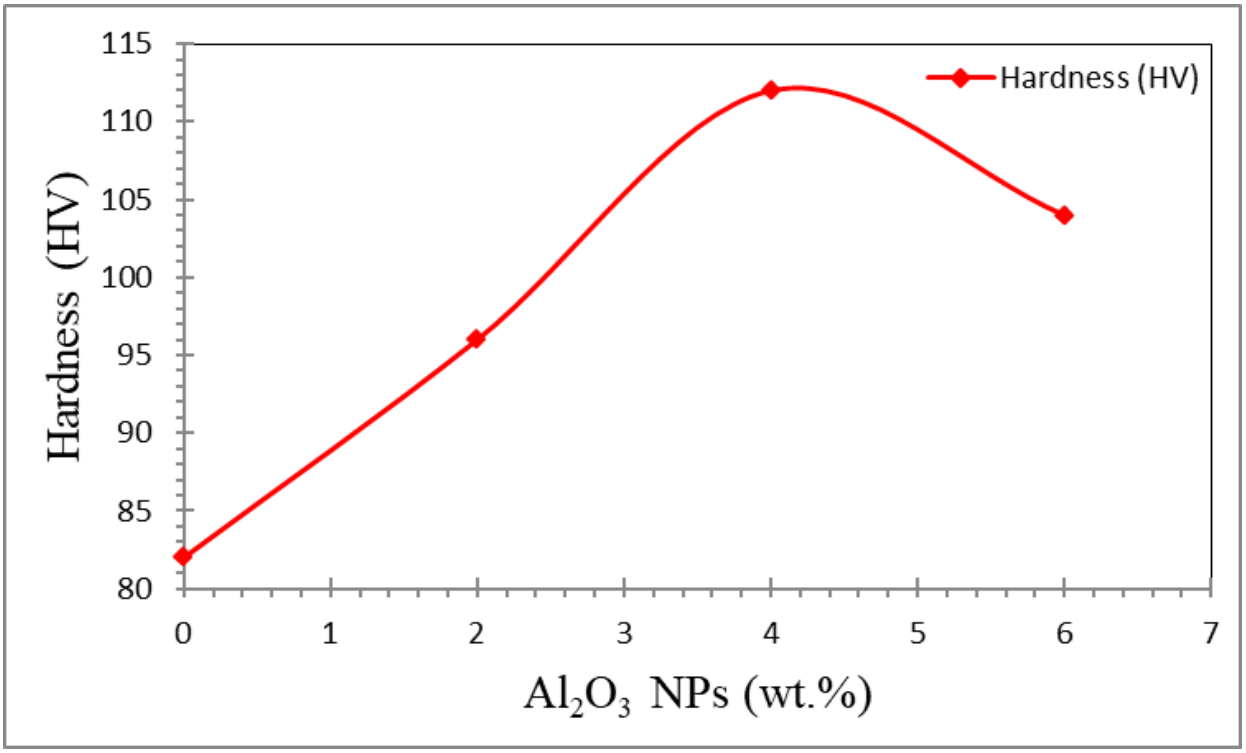

Figure 7 Variation of Vickers hardness of Al– Al_2O_3 NP composites with different Al_2O_3 NP weight fractions, showing maximum hardness at 4 wt.% reinforcement.

3.3.Impact strength behavior of Al–Al_2O_3 NP composites

The impact strength of the Al–Al_2O_3 NP composites is expected to depend strongly on nanoparticle content. At lower reinforcement levels, especially 2 wt.% and 4 wt.%, impact strength may improve

due to better load distribution and enhanced matrix strengthening. However, excessive addition of Al_2O_3 NPs at 6 wt.% may reduce impact strength because of particle agglomeration, increased brittleness, and porosity. These defects act as crack initiation sites and reduce the material's ability to absorb impact energy before fracture [44].

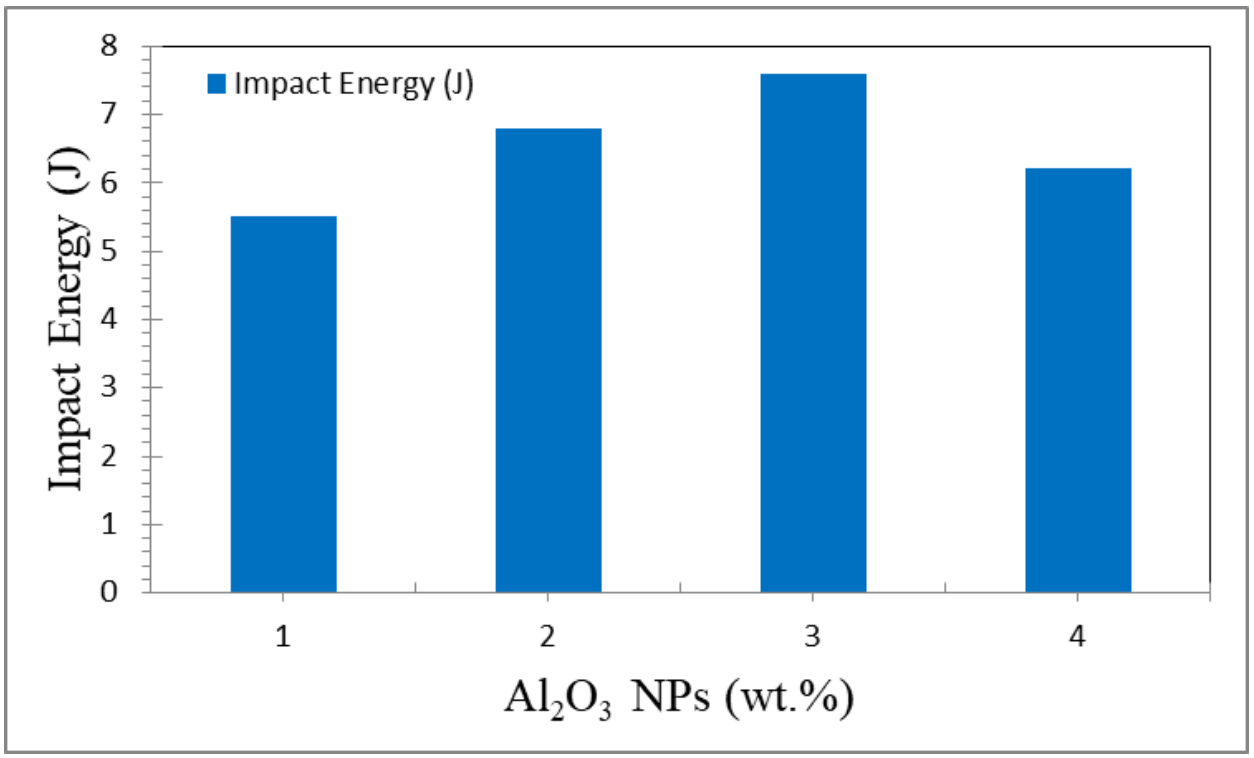

Figure 8 Variation of impact energy of Al–Al_2O_3 NP composites with different Al_2O_3 NP weight fractions, showing maximum impact resistance at 4 wt.% reinforcement.

4. CONCLUSIONS

This study investigated the enhancement of mechanical properties of an aluminum piston alloy (EN AB-47100, AlSi12Cu1) through the incorporation of Al_2O_3 NPs using the stir casting technique. The results demonstrated that the addition of Al_2O_3 NPs significantly improves the tensile strength, hardness, and impact resistance of the alloy, with the degree of improvement strongly dependent on the reinforcement content. Tensile strength increased progressively with the addition of nanoparticles up to 4 wt.%, indicating effective load transfer and strengthening of the aluminum matrix through mechanisms such as dislocation hindrance, Orowan strengthening, and grain refinement. A similar trend was observed for hardness, where the resistance to localized plastic deformation improved due to the presence of hard ceramic nanoparticles uniformly distributed within the matrix. The impact strength also showed improvement at lower reinforcement levels (2 wt.% and 4 wt.%), reflecting enhanced energy absorption capability. However, at higher reinforcement content (6 wt.% Al_2O_3 NPs), a decline in mechanical properties was observed. This reduction was attributed to nanoparticle agglomeration, increased porosity, and poor interfacial bonding, which act as stress concentration sites and promote premature failure. Based on the overall performance, 4 wt.% Al_2O_3 NPs was identified as the optimal reinforcement level, providing the best balance between strength, hardness, and impact

resistance. These findings highlight the potential of Al– Al_2O_3 NP composites for improved durability and performance in piston applications under demanding service conditions.

References

[1] F. Boudou, et al., Not. Sci. Biol. 17 (2025) 12593. https://doi.org/10.55779/nsb17312593
[2] H. K. Aity, E. Dhahri, M. Rasheed. Ceram. Int. 50 (2024) part B 54666. https://doi.org/10.1016/j.ceramint.2024.10.324
[3] I.M. Mohammed, M. Rasheed, AIP Conf. Proc. 3321 (2025) 020026. https://doi.org/10.1063/5.0289719
[4] A. Khaleefah, M. RASHEED, Experimental and Theoretical NANOTECHNOLOGY, 10 (2026) 289. https://doi.org/10.56053/10.s.289.
[5] H. K. Aity, M. Rasheed, E. Dhahri, A. A. Hateef, T. Saidani, Journal of Materials Science, 61 (2026) 6226. https://doi.org/10.1007/s10853-026-12241-w.
[6] D. Kherifi, A. Keziz, M. Rasheed, A. Oueslati. Ceram. Int. 50 (2024) 30175. https://doi.org/10.1016/j.ceramint.2024.05.317
[7] E. Arif, R. Jamal, M. RASHEED, Experimental and Theoretical NANOTECHNOLOGY, 10 (2026) 453. https://doi.org/10.56053/10.2.453
[8] H. Zhang, Y. Li, X. Chen, J. Mater. Res. Technol. 25 (2023) 4120. https://doi.org/10.1016/j.jmrt.2023.06.012.
[9] I. Alshalal, H. M. I. Al-Zuhairi, A. A. Abtan, M. Rasheed, M. K. Asmail. J. Mech. Behav. Mater. 32 (2023) 1. https://doi.org/10.1515/jmbm-2022-0280
[10] F. Boudou, A. Belakredar, A. Berkane, M. Rasheed. Not. Sci. Biol. 17 (2025) 12183. https://doi.org/10.55779/nsb17212183
[11] E. Kadri, K. Dhahri, R. Barillé, M. Rasheed. Phase Transi. 94 (2021) 65. https://doi.org/10.1080/01411594.2020.1832224
[12] A.J. Hussein, M.N. Al-Darraji, M. Rasheed, M.A. Sarhan, IOP Conf. Ser.: Earth Environ. Sci. 1262 (2023) 022007. https://doi.org/ 10.1088/1755-1315/1262/2/022007
[13] A.J. Hussein, M.N. Al-Darraji, M. Rasheed, M.A. Sarhan, IOP Conf. Ser.: Earth Environ. Sci. 1262 (2023) 022005. https://doi.org/10.1088/1755-1315/1262/2/022005
[14] A. Kumar, R. Singh, S. Sharma, Mater. Today Proc. 72 (2023) 2150. https://doi.org/10.1016/j.matpr.2023.02.115
[15] F. Boudou, A. Guendouzi, A. Belkredar. M. Rasheed, Not. Sci. Biol. 16 (2024) 13837. https://doi.org/10.55779/nsb16211837
[16] F. Dkhilalli, S. M. Borchani, M. Rasheed, R. Barille, K. Guidara, M. Megdiche, J. Mater. Sci. Mater. Electron, 29 (2018) 6297. https://doi.org/10.1007/s10854-018-8609-z
[17] J. Chen, H. Zhao, Compos. Part B Eng. 268 (2024) 111066. https://doi.org/10.1016/j.compositesb.2023.111066
[18] K. Patel, R. Patel, J. Mater. Eng. Perform. 32 (2023) 4567. https://doi.org/10.1007/s11665-023-07845-2
[19] L. Wang, Q. Zhou, Mater. Chem. Phys. 301 (2024) 127623. https://doi.org/10.1016/j.matchemphys.2023.127623
[20] M. A. Ali, S. H. Ahmed, Results Eng. 21 (2024) 101695. https://doi.org/10.1016/j.rineng.2024.101695
[21] M. A. Sarhan, S. Shihab, B. E. Kashem, M. Rasheed, J. Phy.: Conf. Ser., 1879 (2021) 022122. https://doi.org/10.1088/1742-6596/1879/2/022122
[22] M. Enneffatia, M. Rasheed, B. Louati, K. Guidara, S. Shihab, R. Barillé, J. Phys.: Conf. Ser. 1795 (2021) 012050. https://doi.org/10.1088/1742-6596/1795/1/012050

[23] M. M. Najim, B. A. Yousif, M. RASHEED, Experimental and Theoretical NANOTECHNOLOGY, 10 (2026) 551. https://doi.org/10.56053/10.2.551
[24] M. M. Najim, B. A. Yousif, M. RASHEED, Experimental and Theoretical NANOTECHNOLOGY, 10 (2026) 627. https://doi.org/10.56053/10.2.627
[25] M. R. Ghanem, M. A. El-Sayed, Alex. Eng. J. 67 (2023) 215. https://doi.org/10.1016/j.aej.2022.11.021
[26] M. Rasheed et al., J. Phys.: Conf. Ser. 1999 (2021) 012080. https://doi.org/10.1088/1742-6596/1999/1/012080
[27] M. RASHEED, A. Khaleefah, Materials Chemistry and Physics, 353 (2026) 132112. https://doi.org/10.1016/j.matchemphys.2026.132112
[28] M. Rasheed, et al., J. Adv. Biotechnol. Exp. Ther. 6 (2023) 495. https://doi.org/10.5455/jabet.2023.d144
[29] M. Rasheed, I. Alshalal, A.A. Ashed, M.A. Sarhan, A.S. Jaber, Indones. J. Electr. Eng. Comput. Sci. 33 (2024) 653. https://doi.org/10.11591/ijeecs.v33.i1.pp653-660
[30] M. Rasheed, M. N. Mohammedali, F. A. Sadiq, M. A. Sarhan, T. Saidani. J. Optics (New Delhi. Print) 54 (2024) 3490. https://doi.org/10.1007/s12596-024-01928-5
[31] M. Rasheed, M. Nuhad Al-Darraji, S. Shihab, A. Rashid, T. Rashid. J. Phys.: Conf. Ser. 1963 (2021) 012058. https://doi.org/10.1088/1742-6596/1963/1/012058
[32] M. Rasheed, M.N. Al-Darraji, S. Shihab, A. Rashid, T. Rashid, J. Phys.: Conf. Ser. 1963 (2021) 012059. https://doi.org/10.1088/1742-6596/1963/1/012059
[33] M. Rasheed, O. Alabdali, S. Shihab, A. Rashid, T. Rashid, J. Phys.: Conf. Ser. 1999 (2021) 012078. https://doi.org/10.1088/1742-6596/1999/1/012078
[34] M. Rasheed, O. Alabdali, S. Shihab, J. Phy.: Conf. Ser. 1879 (2021) 032120. https://doi.org/10.1088/1742-6596/1879/3/032120.
[35] M. Rasheed, O.Y. Mohammed, S. Shihab, A. Al-Adili, J. Phys.: Conf. Ser. 1795 (2021) 012043. https://doi.org/10.1088/1742-6596/1795/1/012043
[36] M. Rasheed, R. Barillé, J. Non-Cryst. Solids., 476 (2017) 1. https://doi.org/10.1016/j.jnoncrysol.2017.04.027
[37] M. Rasheed, R. Barillé, Opt. Quantum Electron. 49 (2017). https://doi.org/10.1007/s11082-017-1030-7
[38] M. Rasheed, S. Shihab, O. Alabdali, A. Rashid, T. Rashid, J. Phys.: Conf. Ser. 1999 (2021) 012077. https://doi.org/10.1088/1742-6596/1999/1/012077
[39] M. Rasheed, SuhaShihab, O. Alabdali, H. H. Hassan, J. Phys. Conf. Ser., 1879 (2021) 032113. https://doi.org/10.1088/1742-6596/1879/3/032113
[40] M. S. El-Kady, A. M. Abdelkader, J. Alloy. Compd. 929 (2023) 167305. https://doi.org/10.1016/j.jallcom.2022.167305
[41] M. Sellam, M. Rasheed, S. Azizi, T. Saidani. Ceram. Int. 50 (2024) 20917. https://doi.org/10.1016/j.ceramint.2024.03.094
[42] N. Assoudi et al. Opt. Quant. Electron. 54 (2022) 9. https://doi.org/10.1007/s11082-022-03927-x
[43] N. Ben Azaza et al., Opt. Mater., 96 (2019) 109328. https://doi.org/10.1016/j.optmat.2019.109328
[44] O. Alabdali, S. Shihab, M. Rasheed, T. Rashid. 3rd inter. Scient. conf. alkafeel univ. (ISCKU 2021) 2386 (2022) 050019. https://doi.org/10.1063/5.0066860
[45] P. S. Rana, D. Chauhan, Mater. Today Commun. 34 (2023) 105034. https://doi.org/10.1016/j.mtcomm.2023.105034
[46] R. Jalal, S. Shihab, M.A. Alhadi, M. Rasheed, J. Phys.: Conf. Ser. 1660 (2020) 012090. https://doi.org/10.1088/1742-6596/1660/1/012090

[47] R. Kumar, A. Gupta, Surf. Coat. Technol. 474 (2024) 129005. https://doi.org/10.1016/j.surfcoat.2023.129005
[48] R.S. Mahmood et al. J. Mech. Behav. Mater. 34 (2025) 1. https://doi.org/10.1515/jmbm-2025-0040
[49] S. K. Verma, P. K. Singh, Mater. Sci. Eng. A 856 (2023) 144041. https://doi.org/10.1016/j.msea.2022.144041
[50] S. R. Das, B. Behera, J. Alloy. Compd. 941 (2024) 168980. https://doi.org/10.1016/j.jallcom.2023.168980
[51] S. S. Batros, M. Rasheed, H. K. Aity, A. A. Hatef, T. Saidani, Materials Chemistry and Physics, 355 (2026) 132243. https://doi.org/10.1016/j.matchemphys.2026.132243
[52] S. Shihab, M. Rasheed, O. Alabdali, A.A. Abdulrahman, J. Phys.: Conf. Ser. 1879 (2021) 022120. https://doi.org/10.1088/1742-6596/1879/2/022120
[53] T. Nguyen, D. Tran, J. Compos. Mater. 57 (2023) 1985. https://doi.org/10.1177/00219983231123456
[54] T. Rashid, M. M. Mokji, M. Rasheed. J. Optics 54 (2024) 3490. https://doi.org/10.1007/s12596-024-02080-w
[55] T. Rashid, M.M. Mokji, M. Rasheed, J. Mech. Behav. Mater. 34 (2025) 77. https://doi.org/10.1515/jmbm-2025-0074
[56] T. Saidani, M. Rasheed, I. Alshalal, A.A. Rashed, M.A. Sarhan, R. Barillé, Res. Eng. Struct. Mater. 10 (2024) 743. http://dx.doi.org/10.17515/resm2023.21ma0922rs
[57] T. Saidani, S. Mokhtari, M. Rasheed, H. Lahmar, M. Trari, Journal of the Indian Chemical Society, 103 (2026) 102499. https://doi.org/10.1016/j.jics.2026.102499
[58] Y. Liu, Z. Wu, Mater. Today Proc. 86 (2024) 1025. https://doi.org/10.1016/j.matpr.2024.01.122.
[59] Z. S. Ahmed, M. RASHEED, H. S. Ahmed, Experimental and Theoretical NANOTECHNOLOGY, 10 (2026) 329. https://doi.org/10.56053/10.s.329
[60] Z. S. Ahmed, M. RASHEED, H. S. Ahmed, Experimental and Theoretical NANOTECHNOLOGY, 10 (2026) 343. https://doi.org/10.56053/10.s.343
[61] A.H. Ali, A.S. Jaber, M.T. Yaseen, M. Rasheed, O. Bazighifan, T.A. Nofal, Complexity 2022 (2022) 1. https://doi.org/10.1155/2022/9367638
[62] A. A. Hateef, E. Dhahri, M. Rasheed, H. Kadhim, Z. Abbas, N. Hassan, Physics and Chemistry of Solid State, 25 (2024) 801. https://doi.org/10.15330/pcss.25.4.801-810
[63] A. R. J. Katae, H. H. Hussein, A. S. Jaber, M. A. Sarhan, M. RASHEED, Experimental and Theoretical NANOTECHNOLOGY, 10 (2026) 357. https://doi.org/10.56053/10.s.357
[64] A. R. J. Katae, H. H. Hussein, A. S. Jaber, M. A. Sarhan, M. RASHEED, Experimental and Theoretical NANOTECHNOLOGY, 10 (2026) 795. https://doi.org/10.56053/10.2.795
[65] A. Boumezoued, K. Guergouri, Régis Barillé, Rechem Djamil, Mourad Zaabat, M. Rasheed, J. Alloys Compd. 791 (2019) 550. https://doi.org/10.1016/j.jallcom.2019.03.251
[66] A. Zubaidi, L.M. Asaad, I. Alshalal, M. Rasheed, J. Mech. Behav. Mater. 32 (2023) 1. https://doi.org/10.1515/jmbm-2022-0302
[67] A. Hassan, M. A. Rahman, Eng. Sci. Technol. Int. J. 38 (2024) 101381. https://doi.org/10.1016/j.jestch.2023.101381
[68] A. Keziz, M. Heraiz, F. Sahnoune, M. Rasheed, Ceram. Int. 49 (2023) 32989. https://doi.org/10.1016/j.ceramint.2023.07.275
[69] A. Keziz, M. Heraiz, M. RASHEED, A. Oueslati. Mater Chem. Phys. 325 (2024) 129757. https://doi.org/10.1016/j.matchemphys.2024.129757
[70] A. Raghdi, M. Heraiz, M. Rasheed, A. Keziz, Journal of the Indian Chemical Society, 101 (2024) 101413. https://doi.org/10.1016/j.jics.2024.101413

[71] A. Jaber, M. Ismael, T. Rashid, M. A. Sarhan, M. Rasheed, I. M. Sala. Eureka: Phys. Eng. 4 (2023) 29. https://doi.org/10.21303/2461-4262.2023.002770
[72] A. I. A. Ali, M. RASHEED, Experimental and Theoretical NANOTECHNOLOGY, 10 (2026) 277. https://doi.org/10.56053/10.s.277
[73] A. I. A. Ali, M. RASHEED, Experimental and Theoretical NANOTECHNOLOGY, 10 (2026) 239. https://doi.org/10.56053/10.s.239
[74] D. Bouras, M. Rasheed, Opt. Quantum Electron. 54 (2022) 12. https://doi.org/10.1007/s11082-022-04161-1